

Length-Dependent Containment of a Pure Electron-Plasma Column

C. F. Driscoll and J. H. Malmberg

Department of Physics, University of California, San Diego, La Jolla, California 92093

(Received 23 July 1982)

The long-time containment of pure electron-plasma columns has been found to depend strongly on the plasma length L , as well as on the axial magnetic field B . Plasma evolution times are observed to scale as $(L/B)^{-2}$ over a range of more than five decades. This transport is probably caused by small azimuthal asymmetries in the applied magnetic or electric fields.

PACS numbers: 52.55.Ke, 52.25.Fi

Pure electron plasmas are one of the simplest systems on which plasma transport effects can be studied.^{1,2} For the experiments reported here, a cylindrical column of electrons is contained by an axial magnetic field B , and by negative potentials applied at the ends of the column. Since the axial containment is energetically assured, the plasma is lost only by radial transport across the magnetic field. Radial transport is constrained by conservation of the total canonical angular momentum of the electrons; this implies that torques from outside the plasma are required for plasma expansion and loss.³ In experiments at background pressures above 10^{-6} Torr, torques from electron-neutral collisions are typically the dominant loss mechanism.^{4,5} However, in experiments at pressures down to 10^{-10} Torr, it has been established that there is also an "anomalous" loss which is independent of background pressure.⁶

Here, we present data showing that this anomalous transport depends strongly on the length L of the plasma column. At base pressures, the length-dependent transport is observed at all experimentally accessible lengths and magnetic field strengths: the transport rate scales approximately as L^2/B^2 over more than five decades. We believe that this transport is caused by small azimuthal asymmetries in the applied magnetostatic or electrostatic fields. Since all physical containment devices will have asymmetries, we believe that this transport will be generic to all nonneutral plasma experiments.⁷ Further, transport due to asymmetric fields is thought to be important in neutral plasma devices such as tandem mirrors.⁸⁻¹⁰ For perspective, we present our transport data in terms of the parameters of single-particle resonant transport theory.

The cylindrical pure-electron-plasma containment apparatus is shown schematically in Fig. 1. The electrostatic boundary is a conducting wall at

radius $R_w = 3.05$ cm. The wall consists of a series of electrically isolated cylinders, some of which are further divided into sectors of various azimuthal extent $\Delta\theta$. The gate cylinders are 6.1 cm in length, the sectors and rings are 3.05 cm, L1 and L2 are 66 and 22.2 cm, respectively, and the interelectrode gaps are 1.27 mm. The entire apparatus is in a uniform static axial magnetic field which is varied over the range $42 \leq B \leq 676$ G. At present, the device operates at a base pressure $P = 5 \times 10^{-10}$ Torr.

The system is normally operated in an inject, hold, dump/measure cycle.⁵ Electrons emitted from a tungsten filament are trapped between a dump gate (e.g., L2) and an injection gate (e.g., G1), by sequential application of negative voltages. The trapped plasma typically has initial central density $n_0 = 1.4 \times 10^7$ cm⁻³, radius $R_p = 1.4$ cm, and length $6.1 \leq L \leq 114$ cm (depending on the choice of injection and dump gates). The average thermal energy is estimated to be 1 eV, on the basis of measurements on similar devices; however, the present apparatus is not instrumented for velocity analysis. The Debye shielding length is typically $\lambda_D = 2$ mm, so that the plasma is many Debye lengths across. The plasma is rotating, since the radial electric field due to space charge gives and $\vec{E} \times \vec{B}$ drift in the $\hat{\theta}$ direction.

After a variable containment time, the dump gate is pulsed to ground potential, allowing the remaining electrons to stream out axially along the field lines to the electrodes where they are collected and measured. The inject/hold/dump cycle may be repeated up to 60 times per second

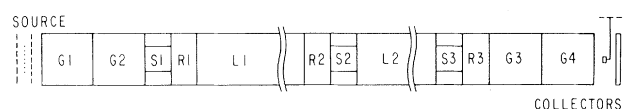


FIG. 1. The cylindrical containment apparatus.

with nearly identical injection conditions, allowing the time evolution of the plasma to be constructed from many separate measurements with differing containment times. We typically characterize this plasma evolution by the time τ_m required for the initial central density to decrease by a factor of 2, and by the time $\tau_{1/2}$ required for one-half of the injected electrons to be lost to the wall.

Recent containment experiments have established that the containment times depend strongly on the length of the plasma column, as well as on the magnetic field. Figure 2 shows the dependence of $\tau_{1/2}$ and τ_m on length, for three magnetic fields. A strong length dependence is observed over the entire range of experimentally accessible lengths and magnetic fields.⁷ The early-time evolution measure τ_m scales approximately as $L^{-2}B^2$. The loss time $\tau_{1/2}$ shows a similar dependence on length and field; however, the scaling of $\tau_{1/2}$ is complicated by the fact that the plasma may have evolved through a wide range in density and temperature by the time $\tau_{1/2}$.

The range of the early-time transport scaling is shown more clearly in Fig. 3, where we plot τ_m vs L/B for all plasma lengths and magnetic fields studied. The data scale as $(L/B)^{-2}$ over more than five decades, with approximately one

decade of scatter. The dashed lines in Figs. 2 and 3 represent

$$\tau_m = 1.6 \times 10^{-2} (L/B)^{-2}, \tag{1}$$

which is the best (slope = -2) fit to the log-log plot. When plotted as a function of the single parameter L/B , the transport data show a striking continuity over the range of evolution times from 3×10^{-3} to 10^3 sec.

Within this length scaling, there are reproducible irregularities. Different containment volumes with equal lengths can show substantially different containment times. For example, three different volumes of length 6.1 cm were measured (G2, G3, S1 + R1), and the containment times differ by as much as a factor of 10. In general, containment volumes which include sectored cylindrical sections have shorter containment times than do equal-length volumes without sectored sections. There are also significant differences in the nature of the transport in different regions of parameter space. These differences are apparent in comparisons of the density profiles $n(r, t)$, and can also be seen by comparing $\tau_{1/2}$ and τ_m in Fig. 2. However, these irregularities seem to be secondary to the fundamental length and magnetic field scalings.

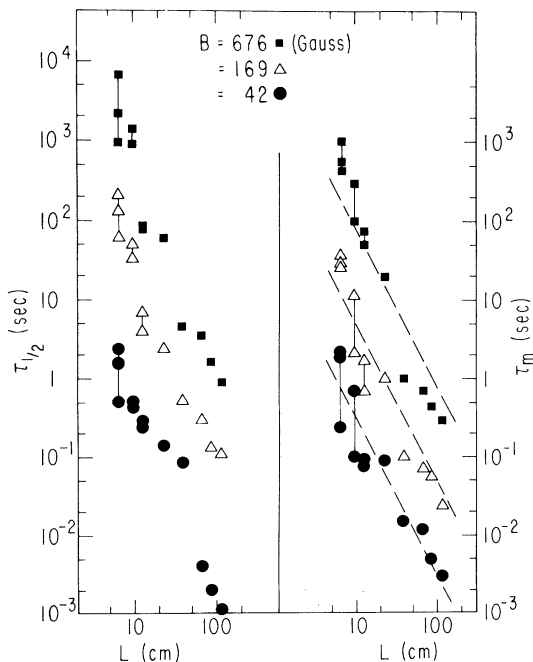


FIG. 2. Dependence of containment times $\tau_{1/2}$ and τ_m on length, for three magnetic fields.

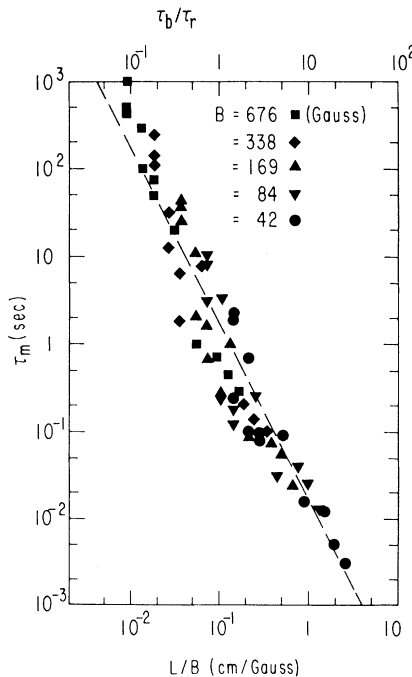


FIG. 3. Measured evolution times τ_m vs L/B for all magnetic fields studied. L/B determines the ratio of bounce time to rotation time, τ_b/τ_r , for an average particle.

The plasma evolution is constrained by conservation of the total canonical angular momentum of the particles. This momentum may be written as

$$P_\theta = \sum_j [mv_{\theta j}r_j - (e/c)A_\theta(r_j)r_j] \approx (-eB/2c)\sum_j r_j^2. \quad (2)$$

Here, the subscript j refers to the j th electron, and $A_\theta(r) = Br/2$ is the vector potential. For the low densities and velocities of our experiments (i.e., $\omega_p \ll \omega_c$ and $v_{\theta j} \ll \omega_c r_j/c$), the kinetic part of the angular momentum is negligible, allowing the approximation shown.³ To the extent that P_θ is conserved, the mean-square radius of the plasma is essentially constant. Radial expansion of the plasma can occur only if torques from outside the plasma change the total angular momentum of the electrons.

At high background pressures ($P \geq 10^{-6}$ Torr), the drag exerted by stationary neutrals on the rotating plasma is the dominant external torque causing plasma expansion and loss. This transport has been studied in detail.⁴⁻⁶ For the plasma parameters of our device, electron-helium collisional transport gives a central evolution time $\tau_m(e-n) = (50 \text{ sec})[B/(42 \text{ G})]^2 [P/(10^{-10} \text{ Torr})]^{-1}$.

At low background pressures, the plasma is lost by an anomalous transport mechanism, which is independent of pressure. An extensive series of experiments has ruled out the possibility that this transport is caused by neutral molecules with exceedingly large momentum-transfer cross section. Experiments further showed that the anomalous loss could not be significantly reduced by tuning the $k_z = 0$ (tilt) and $k_\perp = 2\pi/2L$ (curvature) components of the main magnetic field. Transport due to couplings to electromagnetic radiation¹¹ or due to wave couplings to a resistive wall^{12,13} both seem unlikely on numerical grounds.

The most likely cause of this anomalous transport is small azimuthally asymmetric magnetostatic or electrostatic field errors coupling angular momentum into the plasma. Such field errors would be present in all devices. In our device, magnetostatic errors could arise either from irregularities in the main solenoid, or from induced magnetization of the stainless-steel hangers and rails which support the containment cylinders. (The stainless steel has permeability $\mu \leq 1.005$.) Electrostatic errors could arise from misalignment of the copper cylinders or sectors (typically ± 0.05 mm). Although upper limits to

the error fields can be estimated, we have no direct measurements of the magnitude or spatial distribution of the resulting error fields.

These field asymmetries could couple to the plasma through perturbations to single-particle trajectories, or through collective effects such as diocotron waves. There exists an extensive body of theory treating single-particle resonant transport due to field asymmetries; the main application of these theories has been ion transport in neutral plasma devices such as tandem mirrors.⁸⁻¹⁰ These transport theories consider the bounce, rotation, and collision times of individual particles, and it is interesting to view our data from this perspective.

An average thermal particle bounces axially back and forth in a time $\tau_b = 2L/\bar{v}$. Taking our plasma thermal energy to be 1 eV, the range of containment lengths gives $0.3 \leq \tau_b \leq 5 \mu\text{sec}$. The particle will also experience $\vec{E} \times \vec{B}$ drift around the plasma axis in a time $\tau_r = 2\pi r B/cE(r)$. Taking the electric field near the axis (i.e., using the central density) gives $0.2 \leq \tau_r \leq 3 \mu\text{sec}$ for the experimental magnetic field strengths.

Given an azimuthally asymmetric field error of the form

$$\delta\phi_{p,l}(r) = \cos(p\pi z/L) \cos(l\theta), \quad (3)$$

a particle with axial velocity v and azimuthal rotation time τ_r will remain resonant with the perturbation if $(p\pi/L)v \pm l2\pi/\tau_r = 0$. The resonant particles may make large radial excursions Δr . When collisions interrupt the single-particle drifts, transport proportional to $(\Delta r)^2$ results. For our plasma parameters, the 90° scattering time for electron-electron collisions is approximately 3 msec; of course, a scattering of much less than 90° will generally be sufficient to disrupt a resonant drift orbit. The resonance condition may be rewritten as

$$v/\bar{v} = (l/p)(\tau_b/\tau_r). \quad (4)$$

Since $\tau_b/\tau_r \propto L/B$, the experimental scaling may also be viewed in terms of τ_b/τ_r . For the temperature and density of our experiment, τ_b/τ_r is shown by the upper axis on Fig. 3.

The transport rate scaling as B^{-2} agrees with single-particle resonant transport theory, in which the radial excursions Δr arise from $\vec{E} \times \vec{B}$ drifts and enter as $(\Delta r)^2$. However, the same B^{-2} scaling is common to many transport processes. The L^2 scaling may be obtained from the theory only with *ad hoc* assumptions as to the spectrum

of field errors. From Eq. (4) it can be seen that large τ_b/τ_r requires large p (i.e., short-wavelength errors), in order that the Maxwellian particle distribution be nonzero at the resonant velocity. The data for small τ_b/τ_r are more readily explained by small- p errors, since the theoretical model is suspect at extremely low particle energies. No unifying relation between the two parameter regimes is as yet apparent, and it is surprising that the data scale so regularly over the range in τ_b/τ_r .

We have experimentally verified that azimuthally asymmetric voltages applied to the wall sectors induce radial transport.¹⁴ This transport generally increases with increasing plasma length, and decreases with increasing magnetic field. Magnetostatic perturbations also induce transport, but are less easily manipulated experimentally. We are presently attempting to relate quantitatively the induced transport to the predictions of theory. Correspondence with the naturally occurring transport has not yet been established.

In summary, we have observed pressure-independent particle transport rates scaling as L^2/B^2 over more than five decades. We believe that this transport is caused by small azimuthal asymmetries in the applied magnetic or electric fields. The data are reasonably compatible with single-particle resonant transport theory, but other processes are by no means excluded.

We wish to thank Professor T. M. O'Neil for many useful discussions. This work is based on

research supported by the National Science Foundation under Grant No. PHY80-09326.

¹R. C. Davidson, *Theory of Nonneutral Plasmas* (Benjamin, Reading, Mass., 1974).

²J. H. Malmberg and J. S. deGrassie, *Phys. Rev. Lett.* **35**, 577 (1975).

³T. M. O'Neil, *Phys. Fluids* **23**, 2216 (1980).

⁴M. H. Douglas and T. M. O'Neil, *Phys. Fluids* **21**, 920 (1978).

⁵J. S. deGrassie and J. H. Malmberg, *Phys. Fluids* **23**, 63 (1980).

⁶J. H. Malmberg and C. F. Driscoll, *Phys. Rev. Lett.* **44**, 654 (1980).

⁷Length-dependent transport has also been observed on a second electron-plasma apparatus. This apparatus operates at liquid helium temperatures, has a superconducting coil with 4×10^4 turns, and has no magnetic materials in the containment device.

⁸R. H. Cohen, *Comments Plasma Phys. Controlled Fusion* **4**, 157 (1978).

⁹D. D. Ryutov and G. V. Stupakov, *Dok. Akad. Nauk SSSR* **240**, 1086 (1978) [*Sov. Phys. Dokl.* **23**, 412 (1978)].

¹⁰M. E. Kishinevskij *et al.*, in *Proceedings of the Seventh International Conference on Plasma Physics and Controlled Nuclear Fusion Research, Innsbruck, Austria, 1978* (International Atomic Energy Agency, Vienna, Austria, 1979), Vol. 2, p. 411.

¹¹T. M. O'Neil, *Phys. Fluids* **23**, 725 (1980).

¹²R. J. Briggs, J. D. Daugherty, and R. H. Levy, *Phys. Fluids* **13**, 421 (1970).

¹³W. D. White, J. H. Malmberg, and C. F. Driscoll, *Bull. Am. Phys. Soc.* **26**, 855 (1981).

¹⁴D. L. Eggleston and J. H. Malmberg, *Bull. Am. Phys. Soc.* **27**, 1031 (1982).

Measurements of the Effect of Tokamak Magnetic Field Helicity on Lower Hybrid Resonance Cones

P. M. Bellan

California Institute of Technology, Pasadena, California 91125

(Received 29 November 1982)

The effect of tokamak magnetic field helicity, i.e., rotational transform, on the propagation of lower hybrid resonance cones is clearly observed in the California Institute of Technology Encore tokamak. The observations are in excellent agreement with the predictions of a recent theory.

PACS numbers: 52.35.Fp, 52.40.Fd

Lower hybrid waves are under active investigation as a possible means for driving steady-state dc currents in tokamaks and also for heating tokamak plasmas to fusion ignition. The fundamental behavior of lower hybrid propagation in *straight* magnetic field geometry has been well

established; in particular, it has been shown that lower hybrid waves propagate as *resonance cones*¹⁻³ (described by the cold-plasma, electrostatic two-fluid equations) and that these cones have a fine structure dictated by the geometry of the exciting antenna⁴ and also by higher-order